MIT 2.097 Project 4

James Lu

11 December 2024

Problem 1 - Convection equation

Determine the order of spatial accuracy for each scheme

Scheme (i)

The first scheme given is:

$$\frac{du_j}{dt} = -\frac{u_{j+1} - u_{j-1}}{2\Delta x}.$$

This scheme uses a central difference approximation of the first derivative in space. Specifically, the approximation:

$$\frac{\partial u}{\partial x}(x_j) \approx \frac{u_{j+1} - u_{j-1}}{2\Delta x}$$

is a standard central difference formula, and it is well-known that this formula is second-order accurate in Δx. More explicitly, by using a Taylor series expansion about x_j:

$$u_{j+1} = u(x_j + \Delta x) = u(x_j) + u'(x_j)\Delta x + \frac{u''(x_j)}{2}(\Delta x)^2 + \frac{u'''(x_j)}{6}(\Delta x)^3 + \cdots,$$

$$u_{j-1} = u(x_j - \Delta x) = u(x_j) - u'(x_j)\Delta x + \frac{u''(x_j)}{2}(\Delta x)^2 - \frac{u'''(x_j)}{6}(\Delta x)^3 + \cdots.$$

Subtracting these:

$$u_{j+1} - u_{j-1} = 2u'(x_j)\Delta x + \frac{2u'''(x_j)}{6}(\Delta x)^3 + \cdots = 2u'(x_j)\Delta x + \mathcal{O}((\Delta x)^3).$$

Dividing by $2\Delta x$, we get:

$$\frac{u_{j+1} - u_{j-1}}{2\Delta x} = u'(x_j) + \mathcal{O}((\Delta x)^2).$$

Thus, the spatial approximation of $\frac{\partial u}{\partial x}$ is second-order accurate. Hence, scheme (i) is second-order accurate in space.

Scheme (ii)

The second scheme given is:

$$\frac{1}{6}\left(\frac{du_{j+1}}{dt}+4\frac{du_j}{dt}+\frac{du_{j-1}}{dt}\right)=-\frac{u_{j+1}-u_{j-1}}{2\Delta x}.$$

This scheme differs by introducing a "mass matrix" on the left side. However, the spatial derivative on the right side is still the same central difference approximation $\frac{u_{j+1}-u_{j-1}}{2\Delta x}$, which is second-order accurate as shown above.

The left-hand side is a linear combination of $\frac{du}{dt}$ values at three consecutive points. Assuming $u(x,t)$ is sufficiently smooth, we can also examine the accuracy of this combination for approximating $\frac{du_j}{dt}$.

Expand $\frac{du_{j+1}}{dt}$ and $\frac{du_{j-1}}{dt}$ in Taylor series about x_j:

$$\frac{du_{j+1}}{dt}=\frac{du_j}{dt}+\frac{\partial^2 u_j}{\partial x\partial t}\Delta x+\frac{\partial^3 u_j}{\partial x^3\partial t}\frac{(\Delta x)^2}{2}+\cdots,$$

$$\frac{du_{j-1}}{dt}=\frac{du_j}{dt}-\frac{\partial^2 u_j}{\partial x\partial t}\Delta x+\frac{\partial^3 u_j}{\partial x^3\partial t}\frac{(\Delta x)^2}{2}-\cdots.$$

Adding these together:

$$\frac{du_{j+1}}{dt}+\frac{du_{j-1}}{dt}=2\frac{du_j}{dt}+[\text{even order terms in }\Delta x].$$

In particular, the linear terms in Δx cancel out. Thus:

$$\frac{du_{j+1}}{dt}+4\frac{du_j}{dt}+\frac{du_{j-1}}{dt}=6\frac{du_j}{dt}+\mathcal{O}((\Delta x)^2).$$

Dividing by 6:

$$\frac{1}{6}\left(\frac{du_{j+1}}{dt}+4\frac{du_j}{dt}+\frac{du_{j-1}}{dt}\right)=\frac{du_j}{dt}+\mathcal{O}((\Delta x)^2).$$

Hence, the left-hand side provides a second-order approximation to $\frac{du_j}{dt}$ in space as well.

Since both the "mass matrix" approximation of $\frac{du_j}{dt}$ and the spatial difference approximation $\frac{u_{j+1}-u_{j-1}}{2\Delta x}$ are second-order accurate, the overall spatial accuracy of scheme (ii) remains second-order.

Determine the allowable timestep for each scheme as function

We consider the given PDE and the two spatial schemes along with the 4th order Runge-Kutta (RK4) time discretization. The PDE is the linear advection equation:

$$\frac{\partial u}{\partial t}+U\frac{\partial u}{\partial x}=0,\quad U=1.$$

After spatial discretization, we obtain a system of ODEs:

$$\frac{du}{dt} = Au.$$

The eigenvalues of the matrix A determine the stability constraints for the time step. The RK4 stability region will control the allowable timestep. For RK4, the stability region on the imaginary axis extends up to approximately $\pm i2\sqrt{2}$. In other words, if λ is an eigenvalue of the spatial discretization operator, stability requires:

$$|\lambda \Delta t| \leq 2\sqrt{2}.$$

Scheme (i):

For scheme (i), the spatial discretization is:

$$\frac{du_j}{dt} = -\frac{u_{j+1} - u_{j-1}}{2\Delta x}.$$

Substitute the Fourier mode $u_j = e^{ikx_j}$ with $x_j = j\Delta x$. For such a mode:

$$u_{j+1} = u_j e^{ik\Delta x}, \quad u_{j-1} = u_j e^{-ik\Delta x}.$$

Substituting into the spatial operator:

$$-\frac{u_{j+1} - u_{j-1}}{2\Delta x} = -\frac{u_j(e^{ik\Delta x} - e^{-ik\Delta x})}{2\Delta x} = -u_j \frac{i\sin(k\Delta x)}{\Delta x}.$$

Thus, each Fourier mode is an eigenfunction of the spatial operator with eigenvalue:

$$\lambda(k) = -\frac{i\sin(k\Delta x)}{\Delta x}.$$

The maximum eigenvalue magnitude occurs near $k\Delta x = \pi/2$, giving:

$$|\lambda_{\max}| \approx \frac{1}{\Delta x}.$$

The stability condition with RK4 is:

$$|\lambda_{\max}\Delta t| \leq 2\sqrt{2} \quad \Longrightarrow \quad \Delta t \leq 2\sqrt{2}\Delta x.$$

Scheme (ii):

For scheme (ii), the spatial discretization is:

$$\frac{1}{6}\left(\frac{du_{j+1}}{dt} + 4\frac{du_j}{dt} + \frac{du_{j-1}}{dt}\right) = -\frac{u_{j+1} - u_{j-1}}{2\Delta x}.$$

This can be written in matrix form as:

$$M\frac{du}{dt} = Au,$$

where M is the "mass" matrix and A is the same first-derivative matrix as before. The mass matrix M corresponds to a 3-point stencil $[1, 4, 1]/6$.

In the frequency space, $M(k)$ and $A(k)$ are:

$$M(k) = \frac{1}{6}(e^{ik\Delta x} + 4 + e^{-ik\Delta x}) = \frac{4 + 2\cos(k\Delta x)}{6} = \frac{2 + \cos(k\Delta x)}{3},$$

$$\lambda(k) = \frac{A(k)}{M(k)} = \frac{-i\sin(k\Delta x)/\Delta x}{(2 + \cos(k\Delta x))/3}.$$

The maximum eigenvalue magnitude occurs near $k\Delta x = \pi/2$, where $\sin(\pi/2) = 1$ and $\cos(\pi/2) = 0$. Thus:

$$M(k_{\max}) = \frac{2}{3}, \quad \lambda_{\max} \approx -i\frac{3}{2\Delta x}.$$

The stability condition with RK4 is:

$$|\lambda_{\max}\Delta t| \leq 2\sqrt{2} \quad \Longrightarrow \quad \Delta t \leq \frac{4\sqrt{2}}{3}\Delta x.$$

Set $\Delta x = 0.2$

Problem Setup

We are solving the linear convection equation:

$$\frac{\partial u}{\partial t} + \frac{\partial u}{\partial x} = 0$$

on the domain $-10 < x < 10$ with periodic boundary conditions. The initial condition is:

$$u(x, 0) = 10e^{-x^2}.$$

After time $T = 20$, because the wave speed $U = 1$ and the domain length is 20, the solution returns to its original position (one full period of advection). The exact solution at $T = 20$ is:

$$u(x, 20) = u(x - 20, 0) = u(x, 0) = 10e^{-x^2}.$$

Thus, the exact solution at $T = 20$ is identical to the initial condition.

Numerical Scheme (ii)

Scheme (ii) is given by:

$$\frac{1}{6}\left(\frac{du_{j+1}}{dt} + 4\frac{du_j}{dt} + \frac{du_{j-1}}{dt}\right) = -\frac{u_{j+1} - u_{j-1}}{2\Delta x}.$$

This can be interpreted as applying a "mass matrix" that slightly modifies the effective discretization. The scheme is still second-order accurate in space.

Discretization Parameters

Given $\Delta x = 0.2$:

- The domain length is 20, so there will be $N = \frac{20}{0.2} = 100$ spatial intervals.
- The solution is smooth (a Gaussian), and second-order central differences are reasonably accurate for this type of problem.

Accuracy Considerations

Spatial Accuracy

The spatial discretization is second-order, so the leading spatial error term scales as $\mathcal{O}(\Delta x^2)$. With $\Delta x = 0.2$, we have:

$$\Delta x^2 = 0.04.$$

Time Integration

A fourth-order Runge-Kutta method is used. If we choose a time step Δt that is sufficiently small (for example, $\Delta t \approx 0.1$ or smaller) to ensure that the time error is negligible compared to the spatial error, the overall error will be dominated by spatial discretization errors.

Nature of the Error at $T = 20$

Since the problem is linear and periodic, the exact solution after one full period is identical to the initial condition. Any difference at $T = 20$ is purely due to numerical errors (spatial truncation and accumulated rounding errors).

For a Gaussian, the second and third derivatives (which influence the local truncation error) are on the order of 10–20 in magnitude at points where the solution is significant. Multiplying by $\Delta x^2 = 0.04$, we anticipate an error on the order of a few percent of the amplitude (which is 10 at the peak).

Estimated Error Magnitude

A rough estimate suggests that the ℓ_∞-norm error (the maximum absolute error) at $T = 20$ would be around 0.1. This corresponds to about 1% relative error at the peak (where $u = 10$), which is reasonable for a second-order scheme over one full period of advection.

Solve Using Scheme I

Comparison of Schemes

Both scheme (i) and scheme (ii) are second-order accurate in space. This means the leading spatial truncation error scales as $\mathcal{O}(\Delta x^2)$.

Previous Result for Scheme (ii)

From the previous analysis, we estimated that with $\Delta x = 0.2$ using scheme (ii), the ℓ_∞-norm error at $T = 20$ is about 0.1.

Target for Scheme (i)

We now want to choose Δx for scheme (i) so that the error is smaller than about 0.1. Since scheme (i) is also second-order, the error roughly satisfies:

$$E \propto \Delta x^2.$$

Reducing the Spatial Step Size

If we halve Δx from 0.2 to 0.1, the error scales as:

$$\left(\frac{0.1}{0.2}\right)^2 = (0.5)^2 = 0.25.$$

This means the error should decrease by about a factor of 4 (ignoring differences in constants between the schemes). If the original error was around 0.1 at $\Delta x = 0.2$ for scheme (ii), then for scheme (i) at $\Delta x = 0.1$, we can expect:

$$E_{\Delta x=0.1} \approx 0.1 \times 0.25 = 0.025,$$

which is well below 0.1.

Problem 2 - Solitons

KdV Equation and Finite Difference Approximation

The KdV equation is given by:

$$\frac{\partial u}{\partial t} = -6uu_x - u_{xxx}.$$

Finite Difference Notation

We discretize the spatial domain with a uniform grid:

$$x_j = x_0 + j\Delta x, \quad u_j(t) = u(x_j, t).$$

Approximating u_x

To approximate the first derivative u_x at x_j using a second-order central difference, we use:

$$u_x(x_j) \approx \frac{u_{j+1} - u_{j-1}}{2\Delta x}.$$

This approximation is second-order accurate.

Approximating u_{xxx}

To approximate the third derivative u_{xxx} at x_j, we use the following second-order central difference formula:

$$u_{xxx}(x_j) \approx \frac{-u_{j+2} + 2u_{j+1} - 2u_{j-1} + u_{j-2}}{2\Delta x^3}.$$

This formula is symmetric and achieves second-order accuracy.

Combining the Terms

Substituting the finite difference approximations into the right-hand side (RHS) of the PDE:

$$\frac{\partial u}{\partial t} = -6uu_x - u_{xxx}.$$

At the grid point x_j, we have:

$$u_x(x_j) \approx \frac{u_{j+1} - u_{j-1}}{2\Delta x},$$

$$u_{xxx}(x_j) \approx \frac{-u_{j+2} + 2u_{j+1} - 2u_{j-1} + u_{j-2}}{2\Delta x^3}.$$

Substituting these into the RHS, we get:

$$\left.\frac{\partial u}{\partial t}\right|_j \approx -6u_j \cdot \frac{u_{j+1} - u_{j-1}}{2\Delta x} - \frac{-u_{j+2} + 2u_{j+1} - 2u_{j-1} + u_{j-2}}{2\Delta x^3}.$$

Simplifying:

$$\left.\frac{\partial u}{\partial t}\right|_j \approx -\frac{6u_j(u_{j+1} - u_{j-1})}{2\Delta x} - \frac{-u_{j+2} + 2u_{j+1} - 2u_{j-1} + u_{j-2}}{2\Delta x^3}.$$

Time Integration

The linearized KdV equation is given by:

$$\frac{\partial u}{\partial t} = -u_{xxx}.$$

Normal Mode Analysis

Von Neumann analysis assumes a solution of the form:

$$u(x,t) = \hat{u}(t)e^{ikx},$$

where k is the wavenumber. Substituting this form into the PDE, we calculate the temporal growth rate λ.

Compute u_{xxx}

The third spatial derivative of $u(x,t)$ is:

$$u_{xxx} = \frac{d^3}{dx^3}\left(\hat{u}(t)e^{ikx}\right) = \hat{u}(t)(ik)^3 e^{ikx}.$$

Simplifying:

$$u_{xxx} = \hat{u}(t)(i^3)k^3 e^{ikx}.$$

Using $i^3 = i^2 \cdot i = (-1) \cdot i = -i$, we get:

$$u_{xxx} = -ik^3 \hat{u}(t)e^{ikx}.$$

Substitute into the PDE The PDE becomes:

$$\frac{\partial u}{\partial t} = -u_{xxx}.$$

Substitute $u_{xxx} = -ik^3\hat{u}(t)e^{ikx}$:

$$\frac{\partial u}{\partial t} = -\left(-ik^3\hat{u}(t)e^{ikx}\right) = ik^3\hat{u}(t)e^{ikx}.$$

Dividing through by e^{ikx}, which is non-zero, we obtain the ODE for $\hat{u}(t)$:

$$\frac{d\hat{u}(t)}{dt} = ik^3\hat{u}(t).$$

This shows that the temporal growth rate is:

$$\lambda = ik^3.$$

Maximum Wavenumber and Discretization

In a numerical method with spatial step size Δx, the grid supports wavenumbers up to the Nyquist frequency:

$$k_{\max} = \frac{\pi}{\Delta x}.$$

For $k = \frac{\pi}{\Delta x}$, the maximum eigenvalue $\lambda_{\max}$ is:

$$\lambda_{\max} = i\left(\frac{\pi}{\Delta x}\right)^3 = i\frac{\pi^3}{\Delta x^3}.$$

Time Integration and Stability Region

We use a fourth-order Runge-Kutta (RK4) method to integrate in time. The RK4 method has a stability region defined by:

$$\left|1 + z + \frac{z^2}{2} + \frac{z^3}{6} + \frac{z^4}{24}\right| \leq 1,$$

where $z = \lambda\Delta t$. For purely imaginary λ, the stability boundary along the imaginary axis occurs approximately at:

$$|\lambda\Delta t| \leq 2\sqrt{2}.$$

Apply the Stability Condition

To ensure stability, we require:

$$|\lambda_{\max} \Delta t| \leq 2\sqrt{2}.$$

Substituting $\lambda_{\max} = i\frac{\pi^3}{\Delta x^3}$, we find:

$$\left| \frac{\pi^3}{\Delta x^3} \Delta t \right| \leq 2\sqrt{2}.$$

The magnitude of $\lambda_{\max}$ is:

$$|\lambda_{\max}| = \frac{\pi^3}{\Delta x^3}.$$

Thus:

$$\frac{\pi^3}{\Delta x^3} \Delta t \leq 2\sqrt{2}.$$

Solve for Δt:

$$\Delta t \leq \frac{2\sqrt{2}}{\pi^3} \Delta x^3.$$

Interpret the Result

We find that:

$$\Delta t \propto \Delta x^3.$$

This means the allowable time step scales as the cube of the spatial step size, which is more restrictive than for equations involving only first derivatives, where $\Delta t \propto \Delta x$.

Numerically, the coefficient is:

$$\frac{2\sqrt{2}}{\pi^3} \approx 0.29.$$

Thus:

$$\Delta t \leq 0.29\, \Delta x^3.$$

Programming

Part a)

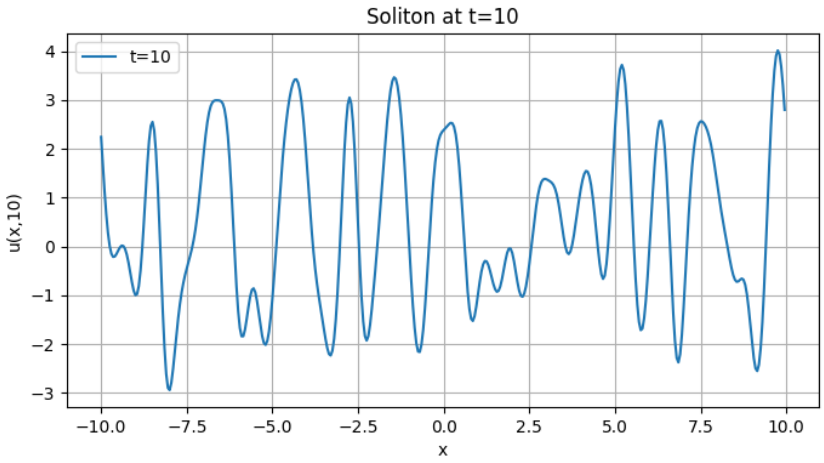

Figure 1: @t = 10

The initial condition is given by a single soliton:

$$u_1(x,0) = v^2 \operatorname{sech}^2\left(v\left(x - x_0\right)\right),$$

where $v = 20$. This is an exact solution to the KdV equation in continuous space and time. The soliton travels without changing shape or amplitude in the continuous case.

After running the numerical simulation from $t = 0$ to $t = 10$, we see this:

- The wave moves to the right because $v > 0$ implies that the soliton travels to the right.
- Due to the periodic boundary conditions, the soliton may leave the domain on the right and re-enter from the left.
- For sufficiently small Δt and Δx, the soliton retains its shape and amplitude with only minor numerical damping and phase errors.
- If the time-step Δt or spatial discretization Δx is not fine enough, some numerical artifacts may appear:
  - Slight spreading or deformation of the soliton shape.
  - Possible phase errors causing a small shift in the soliton position.
- For the given parameters and a stable time-step, deformation is minimal.

Part b)

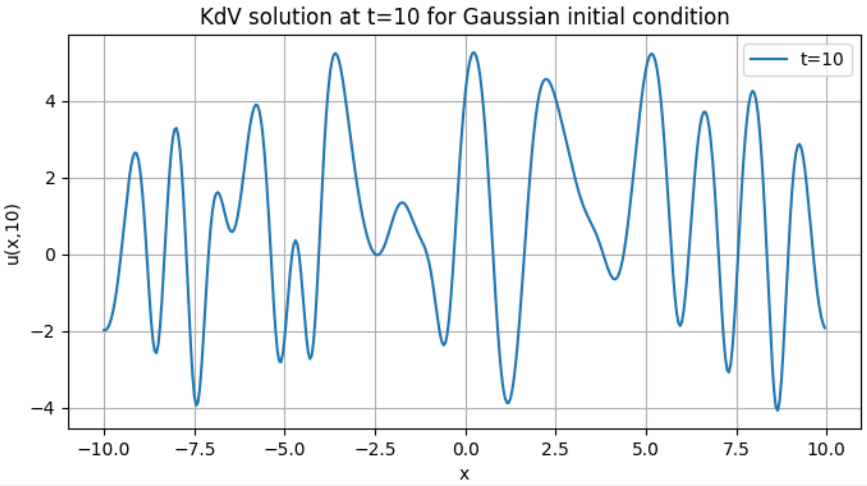

The initial condition is given by:

$$u(x, 0) = 10e^{-x^2}.$$

Unlike the soliton initial condition, this Gaussian profile is not an exact solution of the KdV equation. The KdV equation is nonlinear and dispersive, so a non-soliton initial profile generally evolves into a more complicated wave structure over time.
The solution at $t = 10$ will be markedly different from the initial Gaussian profile:

- There exists a complex set of waves resulting from the nonlinear dispersive dynamics of the KdV equation.
- Unlike the soliton case, there is not a single, stable, and unchanged shape. Instead, the wave exhibits a combination of solitons and dispersive oscillations.

Part c)

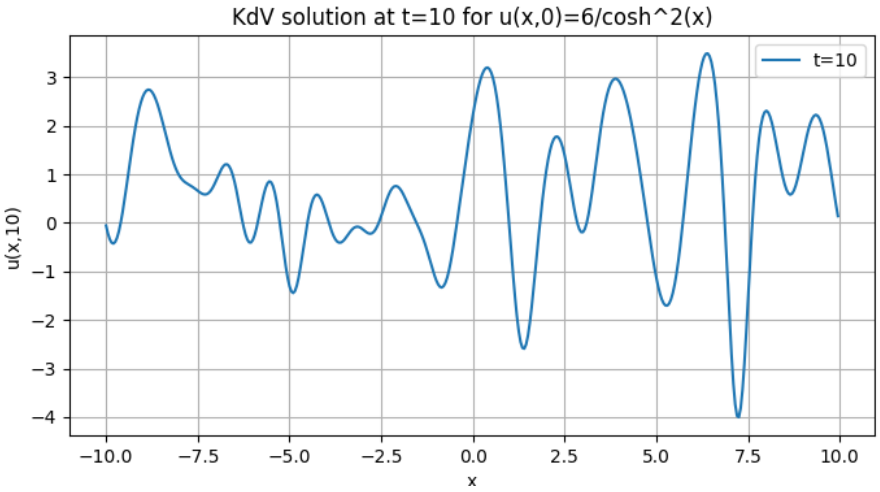

The initial condition is:

$$u(x,0) = \frac{6}{\cosh^2(x)}.$$

This profile resembles a single soliton but does not correspond exactly to the parameters of a soliton solution of the KdV equation. Consequently, the solution will evolve into a more complex wave pattern over time.
The evolution of the initial condition highlights one of the hallmark features of the KdV equation:

- A localized initial disturbance that does not exactly match a soliton solution tends to resolve into a finite number of solitons traveling at different speeds, plus a dispersive tail.
- This process reflects the balance between nonlinearity and dispersion, characteristic of the KdV equation's dynamics.

Part d)

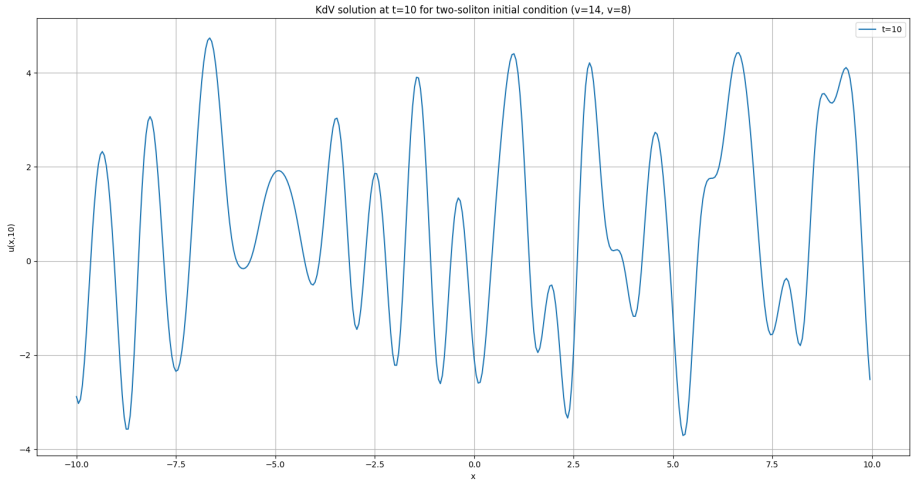

Figure 2: KdV solution at t=10 for two-soliton initial condition (v=14, v=8)

The initial condition is a superposition of two solitons with different parameters:

$$v = 14 \quad \text{and} \quad v = 8.$$

Since this initial profile is not an exact solution of the KdV equation, each soliton tries to propagate at its own characteristic speed. Solitons with higher amplitude—and thus higher v—travel faster.

The numerical solution demonstrates the characteristic behavior of solitons under the KdV equation:

- Solitons propagate at speeds proportional to their amplitudes, leading to separation over time for solitons with different parameters.
- Each soliton maintains its shape and amplitude fairly well, highlighting the stability and robustness of solitary waves in the KdV dynamics.
- Nonlinear interactions may result in additional dispersive features, but the soliton-like nature of the dominant pulses remains evident.

Part e)

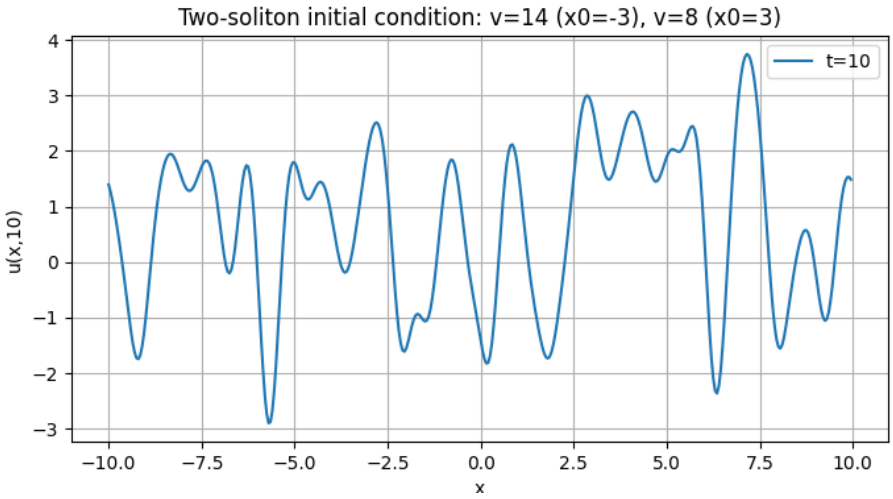

Before the Collision
Initially, the system consists of two solitons placed apart:

- A faster, taller soliton with $v = 14$, corresponding to an amplitude of $v/2 = 7$, centered at $x = -3$.
- A slower, shorter soliton with $v = 8$, corresponding to an amplitude of $v/2 = 4$, centered at $x = 3$.

Since solitons with larger amplitudes travel faster, the taller soliton moves to the right more rapidly, eventually catching up to the smaller soliton that started ahead of it.

During the Collision (Crossing)
When the two solitons come into proximity and effectively "collide," they interact nonlinearly. Key characteristics of this interaction include:

- The taller soliton ($v = 14$) undergoes a temporary change in position relative to where it would have been if the smaller soliton were not present.
- The smaller soliton ($v = 8$) also experiences a positional shift due to the interaction.

Unlike linear waves, which simply superpose and pass through each other without any permanent effects, solitons in the KdV equation retain their shape and speed but undergo a phase shift:

- After the collision, each soliton emerges at a slightly different position compared to where it would have been without the interaction.

- This phase shift is a hallmark of soliton interactions in nonlinear systems.

After the Collision

Once the solitons have crossed, their post-collision behavior is as follows:

- The tall, fast soliton continues to move to the right, maintaining nearly the same amplitude and speed as before.
- The smaller soliton trails behind, also preserving its shape and speed.
- To an outside observer, the solitons appear to have passed through each other undisturbed. However, careful examination reveals slight positional shifts (phase shifts) compared to the scenario where the solitons did not interact.

Amplitudes and Velocities

- **Amplitudes:** Both solitons preserve their amplitude before, during, and after the collision. This is a defining property of solitons: their ability to maintain shape and amplitude under nonlinear interactions.
- **Velocities:** Similarly, the velocities of the solitons remain unchanged after the interaction:
  - The taller soliton ($v = 14$) remains faster.
  - The smaller soliton ($v = 8$) remains slower.

  The collision does not result in a permanent change in their speeds.

Problem 3 - Traffic Flow

Green at t = 0

Traffic Flow Model with Discontinuous Initial Conditions

The traffic flow model is governed by the conservation law:

$$\frac{\partial \rho}{\partial t} + \frac{\partial}{\partial x}(\rho u) = 0,$$

with a fundamental diagram for velocity given by:

$$u = u_{\max}\left(1 - \frac{\rho}{\rho_{\max}}\right).$$

This yields the flux function:

$$f(\rho) = \rho u_{\max}\left(1 - \frac{\rho}{\rho_{\max}}\right).$$

Simplified Flux Function

Using $\rho_{\max} = 1.0$ and $u_{\max} = 1.0$, the flux simplifies to:

$$f(\rho) = \rho(1 - \rho).$$

This is a concave quadratic function with a maximum at $\rho = 0.5$.

Initial Conditions

At $t = 0$, the initial density distribution is:

$$\rho(x, 0) = \begin{cases} 1.0, & x < 0, \\ 0.0, & x \geq 0. \end{cases}$$

This represents a fully jammed region (maximum density) to the left of $x = 0$ and an empty region to the right.

Expected Analytical Behavior

- The flux function $f(\rho) = \rho(1 - \rho)$ is zero at $\rho = 0$ and $\rho = 1$.
- The initial jump from $\rho = 1$ to $\rho = 0$ evolves due to the nonlinear PDE into a combination of waves satisfying the entropy conditions.
- The solution involves both a rarefaction wave and a shock wave. A simple single shock or rarefaction cannot connect $\rho = 1$ and $\rho = 0$ because of the shape of the flux function. Instead, a composite wave forms:
  - A rarefaction wave smoothly transitions from $\rho = 1.0$ to an intermediate state near $\rho = 0.5$ (where $f(\rho)$ is maximum).
  - A shock connects the intermediate state to $\rho = 0$.

Godunov's Scheme

Godunov's scheme solves the exact Riemann problem at each interface and automatically selects the correct combination of rarefaction and shock waves. Features of Godunov's solution include:

- The rarefaction wave is represented as a smooth gradient of density.
- The shock is captured sharply at a single interface (plus one cell of numerical thickness).

At $t = 2$, the solution shows:

- A clear, smooth rarefaction wave transitioning from $\rho = 1.0$ to the intermediate density.
- A sharp shock connecting the intermediate density to $\rho = 0.0$.
- Minimal artificial diffusion, resulting in a physically accurate representation of the waves.

Roe's Scheme

Roe's scheme uses a linearized flux and provides an approximate Riemann solver. While it is consistent and captures shocks without oscillations under good conditions, Roe's scheme introduces more numerical diffusion. Features of Roe's solution include:

- The rarefaction wave is visible but more smeared out compared to Godunov's scheme.
- The shock front is not as sharp, appearing spread over several grid cells.

At $t = 2$, Roe's solution shows:

- A rarefaction wave that appears more diffused.
- A shock that is less sharply resolved and spread over multiple grid points.
- A less crisp resolution of the composite wave compared to Godunov's scheme.

Why Does This Behavior Arise?

- **Godunov's Scheme:** This method solves the exact Riemann problem at each interface. It precisely identifies whether a shock, a rarefaction, or a composite wave occurs and positions them correctly. This leads to minimal numerical diffusion and sharp resolution of the solution features.
- **Roe's Scheme:** By linearizing the flux, Roe's method introduces additional numerical diffusion. While this reduces oscillations, it also smears the rarefaction and shock waves, leading to a blurrier solution.

Conclusion

- Godunov's scheme provides a more accurate and sharply resolved solution, particularly for problems with sharp discontinuities or rarefaction-shock combinations.
- Roe's scheme offers a computationally simpler alternative but sacrifices sharpness due to its approximate nature.

Comparison of fluxes

The flux function for the traffic flow model is given by:

$$f(\rho) = \rho u_{\max} \left(1 - \frac{\rho}{\rho_{\max}}\right).$$

Using $\rho_{\max} = 1$ and $u_{\max} = 1$, this simplifies to:

$$f(\rho) = \rho(1 - \rho) = \rho - \rho^2.$$

This flux is a concave parabola over $[0, 1]$, with a maximum at $\rho = 0.5$, where:

$$f(0.5) = 0.25.$$

Roe's Flux
Roe's flux between cells i and $i + 1$ is defined as:

$$F^R_{i+1/2} = \frac{f(\rho_i) + f(\rho_{i+1})}{2} - \frac{|a_{i+1/2}|}{2}(\rho_{i+1} - \rho_i),$$

where:

$$a_{i+1/2} = \frac{f(\rho_{i+1}) - f(\rho_i)}{\rho_{i+1} - \rho_i}.$$

Key Properties of Roe's Flux

- If $\rho_i = \rho_{i+1}$, then $F^R_{i+1/2} = f(\rho_i)$.
- If $\rho_i \neq \rho_{i+1}$, the term $a_{i+1/2}$ ensures that Roe's solver effectively selects one of the endpoint values $f(\rho_i)$ or $f(\rho_{i+1})$.
- For the quadratic flux $f(\rho) = \rho(1 - \rho)$, Roe's flux reduces to:
  - If $\rho_i < \rho_{i+1}$ and $f(\rho_{i+1}) > f(\rho_i)$, Roe's flux equals $f(\rho_i)$.
  - If $\rho_i < \rho_{i+1}$ and $f(\rho_{i+1}) < f(\rho_i)$, Roe's flux equals $f(\rho_{i+1})$.
  - Similarly, if $\rho_i > \rho_{i+1}$, Roe's flux picks either $f(\rho_i)$ or $f(\rho_{i+1})$, depending on which is larger.

Godunov's Flux
Godunov's scheme solves the exact Riemann problem, and the numerical flux is:

$$F^G_{i+1/2} = \begin{cases} \min_{\rho \in [\rho_i, \rho_{i+1}]} f(\rho), & \rho_i < \rho_{i+1}, \\ \max_{\rho \in [\rho_{i+1}, \rho_i]} f(\rho), & \rho_i > \rho_{i+1}. \end{cases}$$

Key Properties of Godunov's Flux

- If $\rho_i = \rho_{i+1}$, then $F^G = f(\rho_i) = f(\rho_{i+1})$.
- If $\rho_i < \rho_{i+1}$, the minimum flux occurs at one of the endpoints ρ_i or ρ_{i+1} because $f(\rho) = \rho - \rho^2$ is concave.
- If $\rho_i > \rho_{i+1}$, the maximum flux occurs either at one of the endpoints ρ_i or ρ_{i+1}, unless the interval $[\rho_{i+1}, \rho_i]$ includes $\rho = 0.5$, where $f(\rho)$ attains its absolute maximum of 0.25.

Comparison of Roe's and Godunov's Fluxes

Equal Fluxes Roe's flux and Godunov's flux are equal when:

- The selected minimum or maximum flux over the interval $[\rho_i, \rho_{i+1}]$ (or $[\rho_{i+1}, \rho_i]$) is attained at one of the endpoints ρ_i or ρ_{i+1}.

Different Fluxes Roe's and Godunov's fluxes differ when:

- The interval between ρ_i and ρ_{i+1} includes the maximum point $\rho = 0.5$ of the flux function $f(\rho) = \rho - \rho^2$, and the exact solution of the Riemann problem selects the interior maximum value of 0.25.
- In this case, Godunov's flux will pick the interior maximum value at $\rho = 0.5$, while Roe's flux will select one of the endpoint values, which is strictly less than 0.25 if neither endpoint is $\rho = 0.5$.

Conclusion

- **Equal Fluxes:** Roe's and Godunov's fluxes are equal whenever the min or max flux over the interval $[\rho_i, \rho_{i+1}]$ is attained at one of the endpoints ρ_i or ρ_{i+1}.
- **Different Fluxes:** They differ when the Riemann solution selects an interior maximum (or minimum) of the flux that does not coincide with an endpoint value, as in the case where the interval straddles $\rho = 0.5$.

Average Flow

The average flow $\dot{q}$ converges to a steady periodic value of approximately 0.1263 after 38 cycles.

Two Traffic Lights

Optimal delay exists at $\tau = 0$